

Aleksander Hejna^{1,2*}, Mateusz Barczewski¹, Paulina Kosmela², Olga Mysiukiewicz¹

¹ Poznan University of Technology, Institute of Materials Technology, ul. Piotrowo 3, 60-965 Poznan, Poland

² Gdansk University of Technology, Department of Polymer Technology, ul. G. Narutowicza 11/12, 80-233 Gdansk, Poland

*Corresponding author: E-mail: aleksander.hejna@put.poznan.pl

Received (Otrzymano) 25.08.2023

INSIGHTS INTO THE PROCESSING, STRUCTURE, AND MECHANICAL PERFORMANCE OF POLYETHYLENE/GYPSUM COMPOSITES

<https://doi.org/10.62753/ctp.2024.03.1.1>

Polymer composites are used in all branches of industry, with numerous applications. Despite the many years of modifying commodity polymers, using novel fillers allows the range of their applicability to be extended. The impact of new types of fillers on the polymer matrix is not always predictable and requires further studies. The presented study analyzed the application of gypsum as a filler for composites based on high-density polyethylene (PE). The filler was introduced in the amounts of 1-20 wt.%, and its impact on the processing, static, and dynamic mechanical performance of the composites was investigated. At lower filler loadings, the composites could be processed without any hindrance of flowability compared to the neat PE. Up to 5 wt.%, the tensile strength was maintained at a similar level to PE due to the satisfactory quality of the interface and good interfacial adhesion. Higher loadings caused a drop in the tensile strength with a simultaneous rise in Young's modulus. A further increase in the filler loading resulted in higher values of porosity and growth of the adhesion factor, determined from the dynamic mechanical results, which led to deterioration of the mechanical performance.

Keywords: polyethylene, inorganic filler, composite, mechanical properties, dynamic mechanical analysis

INTRODUCTION

Polyethylene (PE), used mainly in the packaging industry [1], is nowadays limited by various law regulations aimed at its replacement with biodegradable polymers [2]. PE is also widely utilized in the construction, agriculture, and electrical industries [3]. The PE market was valued at 103.5 billion USD in 2018, with the forecasts indicating a rise to 143.3 billion USD in 2026 [4]. The multiplicity of PE types and grades enables the preparation of materials with a broad range of properties [5]. Nevertheless, researchers are continuously seeking improvements in PE applications. Two main trends are related to the reduction of its use and the enhancement of PE performance. The first can be realized by applying PE blends with various polymers, often biodegradable ones, or introducing fillers [6]. The manufacturing of composites is also a method to improve performance. The literature review reveals that numerous examples of PE composites reinforced with fibrous- and particle-shaped fillers have been reported, including nanocomposites [7, 8].

Considering the enhancement of the environmental aspects, it is interesting as fillers are various industrial by-products or wastes. Their use has become a subject of scientific interest and a significant trend in industrial practice. Depending on the availability and desired applications, thermoplastic and thermoset polymers are

modified with inorganic and organic waste fillers [9, 10]. Composites reinforced with wood flour or other lignocellulose fillers, called wood-polymer composites, are commonly used in the construction or furniture industry [11].

Nonetheless, their long-term exposure to environmental conditions often limits their use owing to the hydrophilicity and potential decomposition of plant-based materials [12]. To overcome this issue, inorganic waste fillers can be incorporated to improve the sustainability of plant-based composites without affecting their environmental resistance. Even though some examples of inorganic waste fillers such as basalt powder [13] or recycled carbon fiber [14] for thermoplastic composites can be found in the literature, this subject requires deeper insight.

An exciting material that could be applied as a filler for PE is gypsum. In its pure form, it is applied mainly as a raw material in the building industry and manufacturing fertilizers. As a waste, it is often generated as gypsum blocks or gypsum boards during various reconstruction works [15]. Considering its chemical composition, gypsum can be compared to other mineral materials such as limestone, already being investigated as a potential filler for polymer composites [16]. Gypsum has also been applied, mainly for polyester, acrylate

resins, and styrene-butadiene rubber [17]. Among the studies published to date, few studies focus on developing thermoplastic polymer composites by incorporating gypsum as a filler. Ramos and Mendes [18] discuss the possibility of manufacturing composites made of recycled high-density PE (HDPE) and waste lactide gypsum, the by-product of lactic acid fermentation. They focused instead on the structure and thermal properties of the composites rather than the mechanical performance. In another work [19], the effect of the gypsum by-product from flue gas desulfurization as a filler for recycled PE was studied. The authors investigated the performance of highly filled composites (30 to 70 wt.% of filler) compatibilized with maleic anhydride grafted PE (MAGPE). The evaluation of the processing properties by torque rheometry and assessment of the structure-property relationship enabled the production of these composites and their application in the construction industry.

In the mentioned works, the analysis of the static mechanical properties of the composites was related to structural changes caused by gypsum of different origins. While the studies cover a wide range of filler content in PE-based composites, the main focus has been on the fundamental change in the mechanical performance. Therefore, in the presented study, we focused on evaluating the processing and the mechanical properties of PE-based composites filled with gypsum as a filler to assess the possibilities of their utilization in industrial applications. In this work, the focus was additionally on the detailed connection of the formed structural defects resulting from the physicochemical characteristics of the filler with the mechanical properties of the final products assessed under static and dynamic load conditions. Particular attention was paid to the quantitative approach to the dynamic changes in the mechanical properties assessed using the parameters calculated from the dynamic mechanical analysis.

MATERIALS AND METHODS

Materials

HDPE type M300054, with a melt flow index (MFI) of 30 g/10 min (2.16 kg, 190 °C) and density of 0.954 g/cm³ from SABIC, was applied as the matrix to prepare the investigated composites. Gypsum waste filler was obtained from a local store. It was characterized by a bulk density of 2.600 g/cm³.

Preparation of polymer composites

The composites were prepared by melt mixing. First, the HDPE pellets were pulverized into a fine powder using a Tria 25-16/TC-SL high-speed knife grinder. Then, the polymeric powder was preliminarily mixed with 1, 2, 5, 10, or 20 wt.% of gypsum powder. The mixtures were processed by means of a ZAMAK EH16.2D co-rotating twin-screw extruder at

100 rpm with a maximum process temperature of 190 °C. The obtained materials were cooled in forced airflow and pelletized. The resulting composites were then compression molded at 170 °C and 4.9 MPa for 2 min, then kept under pressure at room temperature for 5 min to enable solidification of the material. The unfilled HDPE was processed along with its composites. The samples were named in reference to their filler content as PE and PE/XG, where X stands for the filler content.

Characterization techniques

The melt flow index of the composites was determined at 190 °C, with loads of 1.2, 2.16, and 5 kg, according to ISO 1133:2011, employing a Mflow plastometer from Zwick. Based on the methodology described by Jakubowska et al. [20] and presented in our previous work [21], the rheological characteristics of the obtained composites were determined. The melt viscosity of the sample was calculated according to equation (1):

$$\eta = \zeta / \gamma_w \quad (1)$$

where: ζ – shear stress [Pa]; γ_w – corrected shear rate [1/s]. The shear stress was determined based on equation (2):

$$\zeta = (\Delta p \cdot R) / 2L \quad (2)$$

where: Δp – pressure drop [Pa]; R – capillary radius, 2.095 mm; L – capillary length, 8 mm.

The Rabinowitsch correction of the shear rate was determined according to equation (3):

$$\gamma_w = (3 \cdot n + 1) / (4 \cdot n) \cdot \gamma_a \quad (3)$$

where: n – slope of the line fitted to the data points calculated with by means of equation (4):

$$\log(\zeta) = f(\log(\gamma_a)) \quad (4)$$

The apparent shear rate was calculated by the following equation (5):

$$\gamma_a = (4 \cdot Q) / (\pi \cdot R^3) \quad (5)$$

where Q – volume flow rate [m³·s⁻¹].

The density of the filler and the composites was determined using an Ultrapyc 5000 Foam gas pycnometer from Anton Paar. The following settings were applied: gas – helium; target pressure – 10.0 psi (filler), 18.0 psi (composites); temperature – 20.0 °C; flow mode – fine powder (filler) and monolith (composites); cell size – small, 10 cm³; preparation mode – pulse, four pulses (filler), flow, 0.5 min (composites).

The results of the density measurements were utilized to calculate the theoretical density of the composites and determine their porosity. These parameters were calculated according to the following equation (6) [21]:

$$\rho_{theo} = \rho_m \cdot (1 - \phi) + \rho_f \cdot \phi \quad (6)$$

where: ρ_{theo} – density of the composite [g/cm^3]; ρ_m – density of the matrix [g/cm^3]; ρ_f – density of the filler [g/cm^3]; φ – volume fraction of the filler.

The volume fraction of the gypsum was determined employing equation (7):

$$\varphi = (\theta_f \cdot \rho_f) / ((\theta_f \cdot \rho_f) + (\theta_m \cdot \rho_m)) \quad (7)$$

where: θ_f – mass content of filler [wt.%]; θ_m – mass content of matrix [wt.%].

Using the obtained values of the density, the porosity of the composite was calculated:

$$p = (\rho_{theo} - \rho_{exp}) / \rho_{theo} \quad (8)$$

where: p – porosity of the material [%]; ρ_{exp} – experimental value of the density of the composite [g/cm^3].

The tensile performance was analyzed following the PN-EN ISO 527 standard using a Zwick/Roell Z020 apparatus. The tests were performed at a constant speed of 1 mm/min (elastic modulus) and 20 mm/min (tensile strength and elongation at break). Five type 1BA specimens were analyzed for each sample.

The DMA was conducted on a DMA Q800 TA Instruments apparatus. Specimens with dimensions of 40 mm x 10 mm x 2 mm were analyzed in the single cantilever bending mode at 1 Hz under the temperature rising rate of 4°C/min, ranging from -100 to 100 °C. The DMA analysis was based on the ISO 6721:2019 standard.

The storage modulus values determined by DMA analysis, together with the results of the static tensile tests, were employed to calculate the brittleness of the material, according to equation (9) presented by Brostow et al. [22]:

$$B = 1 / (\varepsilon_b \cdot E') \quad (9)$$

where: B – brittleness [$10^{10} \text{ \%} \cdot \text{Pa}$]; ε_b – elongation at break [%]; E' – storage modulus at 25 °C [MPa].

In their work, Brostow et al. [23] presented and investigated the relationship between the brittleness and toughness of multiple polymeric materials. Based on the obtained results, they quantified this dependence and developed mathematical formula (10), which connects these two parameters:

$$\tau = (b + c \cdot B) / (1 + a \cdot B) \quad (10)$$

where: τ – toughness [J/cm^3]; a, b, c – constants.

This relationship can be presented using the power function, also applied in our previous work [24], which facilitates the interpretation of the results and the dependence between the analyzed parameters because of the reduced number of constants. Therefore, the dependence can be presented using the following equation (11):

$$\tau = d \cdot B^e \quad (11)$$

where: d, e – curve geometry constants.

The DMA results were utilized to calculate the adhesion factor determining the quality of interfacial

adhesion between the matrix and filler [21]. It may be calculated by the following equation (12):

$$A = 1 / (1 - \varphi) \cdot (\tan \delta_c / \tan \delta_m) - 1 \quad (12)$$

where: A – adhesion factor; $\tan \delta_c$ and $\tan \delta_m$ – values of the loss tangent for the composite and the matrix, respectively.

Moreover, the volume of polymer chains constrained by the filler was determined from the DMA results. This volume can be determined, based on literature works [25, 26], employing the following equation (13):

$$C_v = 1 - ((1 - C_0) \cdot W) / W_0 \quad (13)$$

where: C_v – volume fraction of the immobilized polymer chains [%]; C_0 – C_v in pure PE (taken to be 0) [%]; W and W_0 – energy loss fractions for the analyzed sample and pure PE, respectively.

Energy loss fractions W can be calculated from $\tan \delta$ based on the following equation (14):

$$W = (\pi \cdot \tan \delta) / (\pi \cdot \tan \delta + 1) \quad (14)$$

RESULTS AND DISCUSSION

Figure 1 presents the results of the melt flow analysis performed using a different load. At low contents of filler, the flowability of the melt was hardly affected. For sample PE/1G, the values of mass (MFR) and volume flow rates (MVR) were maintained at the level of neat PE. Generally, up to a 5 wt.% content of gypsum, the flowability of the material was hardly affected, which can be considered very beneficial. For samples PE/10P and PE/20P, the decrease in the mass flow rate was in the range of 4.5-5.6 and 10.4-13.3 and relatively higher for the volume flow rate. The values of the melt density express the relationship between the mass and volume flow rates.

For a more detailed analysis of the influence of the gypsum addition on the rheological performance of the composites, Figure 1 shows the relationships between the melt viscosity and corrected shear rate determined according to the equations mentioned above (1)-(5). The viscosity of the analyzed melts grows with the content of gypsum. However, the differences were negligible up to 5 wt.% loadings, confirming the values of the mass and volume flow rates. Moreover, it can be noticed that the dependence between the viscosity and shear rate exhibits a non-linear character, pointing to the shear-thinning behavior of the materials [27]. For such materials, also called pseudoplastic, when shear stress is applied, the particles are arranged along the flow direction until the best possible arrangement is achieved. Therefore, the slope of the lines connecting the data points decreases with the rise in the shear rate [28]. Such an effect is beneficial because it may facilitate the processing of the polymer melts.

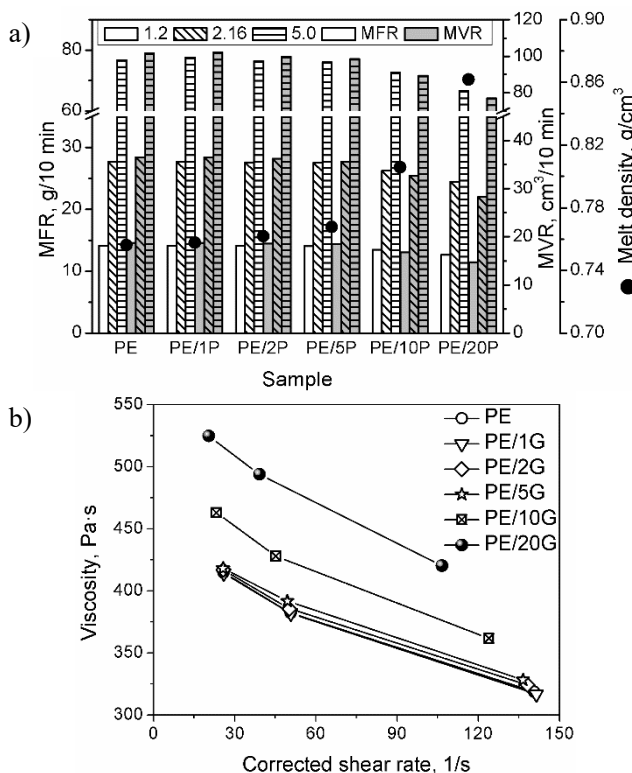
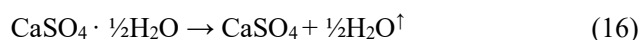
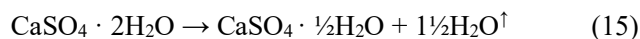


Fig. 1. Plots of MFR, MVR, and melt density of prepared composites (a), and melt viscosity of prepared composites as a function of corrected shear rate (b)

The physical and mechanical properties of the PE/gypsum composites are presented in Table 1. Incorporating solid mineral particles into the PE matrix increased the density of the composites, which was associated with significant differences in the densities of the matrix and filler -0.952 and 2.600 g/cm³, respectively. Such an effect was also observed by other researchers investigating polymer composites with mineral fillers [18].

Porosity is a critical factor for the mechanical performance of composite materials since it quantitatively

determines the number of voids and discontinuity in the material. It directly influences the mechanical performance of the composites thus it must be monitored [29]. In the case of polymer composites, porosity often generates structural imperfections, mainly when insufficient interfacial compatibility is observed. Such an effect may be associated with the differences in the chemical structure and polarity of the components as well as the resulting air inclusions due to the agglomeration of filler particles. The introduction of gypsum also generated porosity in the composite structure, which may further affect the performance of the material. Theoretically, porosity can be generated by the partial decomposition and dehydration of gypsum, whose mechanism is presented in formulas (15) and (16):



Gypsum dehydration takes place in the range of 120–250 °C [30]. It is a two-step process, with the highest decomposition rates around 184 and 205 °C. The raw materials were dried to eliminate the moisture impact before melt compounding was performed at 190 °C. Nevertheless, it is possible that residual moisture was present in the prepared granulates, and applying pressure during compression molding yielded a slightly porous structure. To evaluate the impact of the processing scheme, the amount of water vapor generated according to the above-presented scheme was calculated and compared to the porosity of the prepared sample. The results of calculations made for 100 g of materials are presented in Table 2. During the calculations, it was assumed that the purity of the applied gypsum is 100%, its molar mass equals 172.19 g/mol [31], the molar volume of water vapor is 22.4 dm³/mol [32], and the dehydration of gypsum occurs with 100% yield.

TABLE 1. Physico-mechanical properties of prepared composites

Parameter	PE	PE/1G	PE/2G	PE/5G	PE/10G	PE/20G
Theoretical density [g/cm ³]	0.9517	0.9577	0.9636	0.9828	1.0161	1.0898
Experimental density [g/cm ³]	0.9517	0.9553	0.9605	0.9720	0.9960	1.0547
Porosity [%]	-	0.253	0.350	1.099	1.978	3.224
Filler volume fraction [%]	-	0.37	0.74	1.89	3.91	8.38
Tensile strength [MPa]	23.0 ± 1.1	23.0 ± 1.1	22.4 ± 0.3	21.0 ± 0.3	19.0 ± 1.2	18.0 ± 0.6
Elongation at break [%]	407 ± 54	91.0 ± 14.7	19.0 ± 1.0	13.6 ± 0.8	5.3 ± 0.8	3.6 ± 0.4
Young's modulus [MPa]	917 ± 43	919 ± 27	966 ± 47	1030 ± 41	1104 ± 5	1197 ± 37
Toughness [J/cm ³]	5726 ± 658	1723 ± 118	368 ± 49	276 ± 37	118 ± 27	61 ± 11
Brittleness [10 ¹⁰ %·Pa]	0.0141	0.0745	0.3400	0.4474	1.0892	1.6626
tanδ at 25 °C	0.0597	0.0583	0.0580	0.0584	0.0606	0.0609
tanδ at T _g	0.0503	0.0495	0.0488	0.0482	0.0470	0.0460
T _g [°C]	-111.7	-112.0	-112.6	-113.2	-113.5	-113.7
Adhesion factor at 25 °C	-	-0.190	-0.0219	-0.0029	0.0564	0.1132
Constrained chain volume [%]	0.00	1.37	2.45	3.53	5.62	7.39

TABLE 2. Results of calculations related to water vapor generation during processing of PE/G composites

Parameter	PE/1G	PE/2G	PE/5G	PE/10G	PE/20G
Gypsum content [g]	1.00	2.00	5.00	10.00	20.00
Gypsum content [moles]	0.0058	0.0116	0.0290	0.0581	0.1162
Water vapor generated in 1 st step [moles]	0.0087	0.0174	0.0436	0.0871	0.1742
Water vapor generated in 1 st step [dm ³]	0.1951	0.3903	0.9757	1.9513	3.9027
Water vapor generated in 2 nd step [moles]	0.0029	0.0058	0.0145	0.0290	0.0581
Water vapor generated in 2 nd step [dm ³]	0.0650	0.1301	0.3252	0.6504	1.3009
Total water vapor generated [moles]	0.0116	0.0232	0.0581	0.1162	0.2323
Total water vapor generated [dm ³]	0.2602	0.5204	1.3009	2.6018	5.2036
Density of material [g/cm ³]	0.9553	0.9605	0.9720	0.9960	1.0547
Volume of the 100 g sample [cm ³]	104.679	104.112	102.881	100.402	94.814
Porosity of sample [%]	0.253	0.350	1.099	1.975	3.224
Volume of pores [cm ³]	0.265	0.364	1.131	1.983	3.057
Volume of pores/total water vapor generated [%]	0.102	0.070	0.087	0.076	0.059

The ratio of the total pore volume determined by gas pycnometry to the theoretical volume of water vapor generated during gypsum dehydration is exceptionally low, hardly exceeding 0.1% for sample PE/1G. Even considering the simplifications during the calculations, the drying of the raw materials and their processing were correctly carried out, and the moisture was removed very efficiently. Therefore, the porosity in the prepared composites was probably induced mainly by the agglomeration of the gypsum particles, especially at higher loadings.

The incorporation of gypsum hardly affects the tensile strength of the material. For all the samples, the values ranged from 22.1–23.3 MPa. Enhancement of the strength of the composites was accompanied by increased stiffness, often observed for incorporating solid particles into polymer matrices [21]. The 10 wt.% reduction of the virgin polymer use could be achieved without significantly dropping the material's strength. Considering the economic and ecological aspects, it has a beneficial effect. Incorporating gypsum caused a significant drop in elongation at break, often observed for polymer composites and associated with a disrupted homogeneity and continuity of structure. Due to their solid particles, polymer macromolecules cannot achieve an optimal arrangement along the stretching direction during the test and therefore break relatively earlier.

The results of the tensile tests were used to determine the toughness values of the composites by integrating the stress-strain curves. Toughness represents the total amount of energy the material can absorb or disperse. Ideally, a tough material should be characterized by high tensile strength values and elongation at break. For the prepared composites, the toughness significantly dropped with the gypsum content owing to the drop in elongation at break induced by the porosity, structural discontinuity, and weak interfacial compatibility.

Table 1 presents the DMA results of the prepared composites. The values of storage modulus determined by DMA analysis and the results of the static tensile tests were used to calculate the brittleness of the material. Brittleness is quite similar to toughness, indicating that a material with low brittleness should withstand possibly high stress in the broadest range of strains. Therefore, brittleness stands as the antagonist of toughness. Nevertheless, these parameters are not inversely proportional. Even though elongation at break is considered in both cases, toughness takes into account the tensile strength, while brittleness takes into account the storage modulus determined by DMA analysis. Table 1 reveals that the brittleness noticeably rose with the gypsum loading, which is caused by the significant drop in the ductility of the material expressed by the decrease in elongation at break.

Brostow et al. [23] presented and investigated the relationship between the brittleness and toughness of multiple polymeric materials. As presented above, they connected brittleness and toughness using the rational function. Nonetheless, we prefer the power function due to the limited number of constants, which was also described in our previous work [24]. This type of function facilitates the interpretation of the obtained results and the dependence between the analyzed parameters. Considering the power function, the value of constant d determines the base value of composite toughness, while constant e plays a similar role in brittleness.

Figure 2 presents the brittleness-toughness relationship for the prepared materials, according to Brostow et al. [23]. Its presentation in logarithmic terms may facilitate the interpretation. For the data presented in [23], the values of d and e are 178.38 and -0.984 , respectively. In the presented work, values of 121.74 and -0.946 were obtained. The experimental data indicates that the PE/G composites lie below the literature curve proposed in [23]. Such an effect is associated with

the fact that they investigated the performance of homogenous materials, such as polymers or metals. Therefore, no influence of interfacial adhesion was considered, which plays a crucial role in composite materials and is often weaker than the cohesion of homogenous polymers. Such an effect points to the insufficient compatibility of gypsum with a PE matrix because no reinforcing effect was noted.

The dynamic mechanical analysis may also provide fascinating insights into the stiffness of the material and its damping performance, which are related to the loss tangent ($\tan \delta$) of the material – a parameter related to the material's ability to dissipate energy. Moreover, it can be used to determine the glass transition temperature (T_g) of the material based on the temperature position of the $\tan \delta$ peak. The T_g and $\tan \delta$ at T_g and 25 °C values of the composites are presented in Table 1, together with the other physico-mechanical parameters.

Even though T_g hardly changes after gypsum incorporation, the values of $\tan \delta$ provide exciting insights into the mechanical performance of the composites. At ambient temperature, values of loss tangent decrease up to the 5 wt.% content of gypsum. Such a phenomenon points to a reduction in the mobility of polymer macromolecules [26]. An adverse effect was noted for the 10 and 20 wt.% gypsum contents.

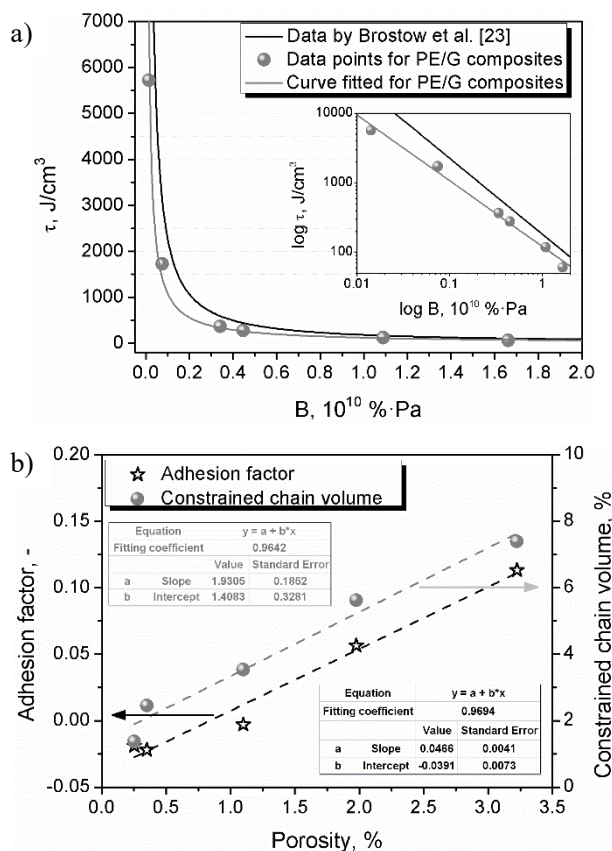


Fig. 2. Plots of (a) toughness-brittleness dependence (a) and porosity impact on A factor and C_v values (b)

The values of $\tan \delta$ may be used for a more in-depth analysis of interfacial adhesion in polymer composites

by calculating the adhesion factor according to the method proposed by Kubat et al. [33]. This idea is associated with the performance of the components of composites – the matrix, filler, and the interface connecting them. The method of adhesion factor calculation was presented in more detail in our previous work [21].

Low values of the A factor indicate strong interfacial adhesion. Because of the simplifications mentioned above, the adhesion factors may even exhibit negative values. It can be seen that the lowest values of the A parameter are noted for the PE/1G and PE/2G composites. A drastic increase is noted for the samples containing 10 and 20 wt.% of gypsum, which confirms the results of the static mechanical tests and the decline in the tensile strength with the increasing filler loading. Such an effect also suggests agglomeration of the filler particles.

Except for the adhesion factor, the values of $\tan \delta$ may be applied to quantify the number of polymer chains immobilized by the filler particles. Reduced mobility of the polymer macromolecules inside the composite may suggest an increment in the number of polymer chains constrained by the filler particles [25]. Their number can be determined using the magnitude of $\tan \delta$ peaks. It can be seen in Table 1 that the values of $\tan \delta$ at T_g fall with the filler content. Such an effect is associated with incorporating solid particles into the polymer and has been confirmed numerically [21]. The calculated C_v values presented in Table 1 grew with the filler loading, but this increase was not proportional. For the PE/1G and PE/2G samples, the C_v values are higher than the mass filler contents. Such an effect is not observed for higher gypsum loadings. At 5, 10, and 20 wt.% contents of filler, the constrained chain volume stands for around 71, 56, and 37 % of the filler content, indicating the filler's reduced ability to immobilize the polymer macromolecules. It can be associated with the agglomeration of filler particles and the interfacial area not proportional to the filler content or the porosity of the composites. The influence of the latter issue on the adhesion factor and constrained chain volume is presented in Figure 2.

It can be seen that these parameters are directly connected and exhibit almost linear dependencies. Such an effect is associated with voids being present mainly at the interface in polymer composites as a consequence of air inclusions during processing and the possible evaporation of residual moisture or volatiles generated from the fillers. Therefore, it is essential to monitor the porosity of composite materials and counteract its formation.

CONCLUSIONS

The presented work investigated the impact of gypsum filler on the processing, structure, and mechanical performance of PE-based composites. The melt flow analysis pointed to the hardly affected flowability of the

polymer melts up to 5 wt.% of filler, enabling the processing of composites with a lower filler content without suppressing the rheological behavior compared to the neat PE matrix. Portions of air were introduced into the structure of the composites during sample preparation, resulting in its slight porosity.

Such an effect, together with the lack of chemical bonding between the phases resulting from the chemical structures of both phases, caused slight deterioration in the mechanical performance of the higher gypsum loadings. Nevertheless, up to the 5 wt.% filler content, only an 8% drop in the tensile strength was observed, with a simultaneous 12% rise in Young's modulus. It was associated with the low values of the adhesion factor, indicating the satisfactory quality of the interface. Higher loadings raised the A factor, indicating weakened interfacial interactions induced by the agglomeration of filler particles. The presented paper comprehensively investigated the static and dynamic mechanical performance of PE/gypsum composites and indicated areas where improvements are necessary.

Based on the obtained data and considering the potential industrial application of the developed composites in the light of current law regulations, future works in the field will aim to evaluate the long-term durability and assess the eco-efficiency based on the environmental impacts and economic aspects of the composites.

Acknowledgments

The work was financed by the Ministry of Education and Science (Poland) under Project 0513/SBAD/4720.

REFERENCES

- [1] Czarnańska-Komorowska D., Wiszumirska K., Sustainability design of plastic packaging for the circular economy, *Polimery* 2020, 65, 8-17, DOI: 10.14314/polimery.2020.1.2.
- [2] Hejna A., Renewable, degradable, and recyclable polymer composites, *Polymers* 2023, 15, 1769, DOI: 10.3390/polym15071769.
- [3] Kasirajan S., Ngouajio M., Polyethylene and biodegradable mulches for agricultural applications: a review, *Agron. Sust. Dev.* 2012, 32, 501-529, DOI: 10.1007/s13593-011-0068-3.
- [4] Fortune Business Insights. *Plastics Polymers & Resins / Polyethylene (PE) Market*, <https://www.fortunebusinessinsights.com/industry-reports/polyethylene-pe-market-101584> 2023.
- [5] Peterlin A., Molecular model of drawing polyethylene and polypropylene, *J. Mater. Sci.* 1971, 6, 490-508, DOI: 10.1007/BF00550305.
- [6] Olesik P., Koziół M., Jała J., Processing and structure of HDPE/glassy carbon composite suitable for 3D printing, *Compos. Theory Pract.* 2020, 20, 72-77.
- [7] Gnatowski A., Kazik E., Palutkiewicz P., Investigation of properties of molded parts made of polyethylene with addition of ash from bituminous coal, *Compos. Theory Pract.* 2018, 18, 127-132.
- [8] Rudawska A., Jakubowska P., Kloziński A., Surface free energy of composite materials with high calcium carbonate filler content, *Polimery* 2017, 62, 434-440, DOI: 10.14314/polimery.2017.434.
- [9] Członka S., Strąkowska A., Kairyte A., Effect of walnut shells and silanized walnut shells on the mechanical and thermal properties of rigid polyurethane foams, *Polym. Test.* 2020, 87, 106534, DOI: 10.1016/j.polymertesting.2020.106534.
- [10] Kairyte A., Kremensas A., Vaitkus S., Członka S., Strąkowska A., Fire suppression and thermal behavior of bio-based rigid polyurethane foam filled with biomass incineration waste ash, *Polymers* 2020, 12, 683, DOI: 10.3390/polym12030683.
- [11] Sałasińska K., Ryszkowska J., Dimensional stability, physical, mechanical and thermal properties of high density polyethylene with peanut hulls composites, *Polimery* 2013, 58, 461-466, DOI: 10.14314/polimery.2013.461.
- [12] Gunjal J., Aggarwal P., Chauhan S., Changes in colour and mechanical properties of wood polypropylene composites on natural weathering, *Maderas Ciencia Tecnol.* 2020, 22, 325-334, DOI: 10.4067/S0718-221X2020005000307.
- [13] Barczewski M., Sałasińska K., Kloziński A., Skórczewska K., Szulc J., Piasecki A., Application of the basalt powder as a filler for polypropylene composites with improved thermo-mechanical stability and reduced flammability, *Polym. Eng. Sci.* 2019, 59, E71-79, DOI: 10.1002/pen.24962.
- [14] Andrzejewski J., Misra M., Mohanty A.K., Polycarbonate biocomposites reinforced with a hybrid filler system of recycled carbon fiber and biocarbon: Preparation and thermo-mechanical characterization, *J. Appl. Polym. Sci.* 2018, 135, 46449, DOI: 10.1002/app.46449.
- [15] Ahmed A., Ugai K., Kamei T., Investigation of recycled gypsum in conjunction with waste plastic trays for ground improvement, *Constr. Build. Mater.* 2011, 25, 208-217, DOI: 10.1016/j.conbuildmat.2010.06.036.
- [16] Guo Y., Jiang K., Bourell D.L., Preparation and laser sintering of limestone PA 12 composite, *Polym. Test.* 2014, 37, 210-215, DOI: 10.1016/j.polymertesting.2014.06.002.
- [17] Kumar S.R., Bhat I.K., Patnaik A., Novel dental composite material reinforced with silane functionalized micro-sized gypsum filler particles, *Polym. Compos.* 2017, 38, 404-415, DOI: 10.1002/pc.23599.
- [18] Ramos F.J.H.T.V., Mendes L.C., Recycled high-density polyethylene/gypsum composites: evaluation of the microscopic, thermal, flammability, and mechanical properties, *Green Chem. Lett. Rev.* 2014, 7, 199-208, DOI: 10.1080/17518253.2014.924591.
- [19] Bilici I., Deniz C.U., Oz B., Thermal and mechanical characterization of composite produced from recycled PE and flue gas desulfurization gypsum, *J. Compos. Mater.* 2019, 53, 3325-3333, DOI: 10.1177/0021998319827097.
- [20] Jakubowska P., Sterzynski T., Samujlo B., Rheological studies of highly-filled polyolefin composites taking into consideration p-V-T characteristics, *Polimery* 2010, 55, 379-389.
- [21] Mysiukiewicz O., Kosmela P., Barczewski M., Hejna A., Mechanical, thermal and rheological properties of polyethylene-based composites filled with micrometric aluminum powder, *Materials* 2020, 13, 1242, DOI: 10.3390/ma13051242.
- [22] Brostow W., Hagg Lobland H.E., Narkis M., Sliding wear, viscoelasticity, and brittleness of polymers, *J. Mater. Res.* 2006, 21, 2422-2428, DOI: 10.1557/jmr.2006.0300.
- [23] Brostow W., Hagg Lobland H.E., Khoja S., Brittleness and toughness of polymers and other materials, *Mater. Lett.* 2015, 159, 478-480, DOI: 10.1016/j.matlet.2015.07.047.
- [24] Galeja M., Hejna A., Kosmela P., Kulawik A., Static and dynamic mechanical properties of 3D printed ABS as a function of raster angle, *Materials* 2020, 13, 297, DOI: 10.3390/ma13020297.

- [25] Bindu P., Thomas S., Viscoelastic behavior and reinforcement mechanism in rubber nanocomposites in the vicinity of spherical nanoparticles, *J. Phys. Chem. B* 2013, 117, 12632-12648, DOI: 10.1021/jp4039489.
- [26] Abdalla M., Dean D., Adibempe D., Nyairo E., Robinson P., Thompson G., The effect of interfacial chemistry on molecular mobility and morphology of multiwalled carbon nanotubes epoxy nanocomposite, *Polymer* 2007, 48, 5662-5670, DOI: 10.1016/j.polymer.2007.06.073.
- [27] Krishnan J.M., Deshpande A.P., Kumar P.B.S., editors. *Rheology of Complex Fluids*, Springer, New York 2010, DOI: 10.1007/978-1-4419-6494-6.
- [28] Hejna A., Piszcz-Karaś K., Filipowicz N., Cieśliński H., Namieśnik J., Marć M., Klein M., Formela K., Structure and performance properties of environmentally-friendly biocomposites based on poly(ϵ -caprolactone) modified with copper slag and shale drill cuttings wastes, *Sci. Total Environ.* 2018, 640-641, 1320-1331, DOI: 10.1016/j.scitotenv.2018.05.385.
- [29] Salasinska K., Polka M., Gloc M., Ryszkowska J., Natural fiber composites: the effect of the kind and content of filler on the dimensional and fire stability of polyolefin-based composites, *Polimery* 2016, 61, 255-265, DOI: 10.14314/polimery.2016.255.
- [30] Ghazi Wakili K., Hugi E., Wullschleger L., Frank T., Gypsum board in fire – modeling and experimental validation, *J. Fire Sci.* 2007, 25, 267-282, DOI: 10.1177/0734904107072883.
- [31] Jin Q., Perry L.N., Bullard J.W., Temperature dependence of gypsum dissolution rates, *Cem. Concr. Res.* 2020, 129, 105969, DOI: 10.1016/j.cemconres.2019.105969.
- [32] Gray J.M., The variable and absolute specific heats of water, *Proc. Inst. Civil Eng.* 1902, 147, 347-376.
- [33] Kubát J., Rigdahl M., Welander M., Characterization of interfacial interactions in high density polyethylene filled with glass spheres using dynamic-mechanical analysis, *J. Appl. Polym. Sci.* 1990, 39, 1527-1539, DOI: 10.1002/app.1990.070390711.